Supplemental Material: First-time observation of Timelike Compton Scattering

P. Chatagnon, S. Niccolai, S. Stepanyan
(Dated: August 9, 2021)

REACTION MECHANISM AND EXCLUSIVITY CUTS

Time-like Compton scattering is studied using a 10.6 GeV electron beam incident on a hydrogen target. Electron scattering is used to study the lepton pair production off of the proton in the reaction:

$$e(\mathrm{e})p(\mathrm{p}) \rightarrow e^{+}(\mathrm{k}^{+})e^{-}(\mathrm{k}^{-})p'(\mathrm{p}')X \tag{1}$$

e, p, k^+, k^-, and p' in parentheses are the four momenta of the initial and final state particles. The quasi-real photoproduction of (e^+e^-) is identified in the missing momentum analysis, by constraining the missing system X to be the scattered electron at $\theta' \sim 0$. The two kinematic constraints used to select the photoproduction reaction are the missing mass squared, $M_X^2 = \mathrm{p}_X^2$, and the missing transverse momentum P_t/P_X, where p_X is the four-momentum of the missing system:

$$\mathrm{p}_X = \mathrm{e} + \mathrm{p} - \mathrm{k}^+ - \mathrm{k}^- - \mathrm{p}' \tag{2}$$

The P_X and P_t are the missing three momentum and its transverse component. The exclusivity cuts used to constrain the photoproduction kinematics are $|M_X^2| < 0.4$ GeV^2 and $P_t/P_X < 0.05$. The two processes contributing to the final state are electroproduction with $Q^2 \sim 0$ and pure photoproduction, when the incident electron emits a real photon via bremsstrahlung, which then interacts with the proton, see Fig.1. The main contribution to the reaction in (1) comes from the left diagram of the figure. The cut on transverse missing momentum, $P_t/P_X = \sin\theta_X < 0.05$, limits the virtuality of the incoming space-like photon to $Q^2 = 2EE_X(1 - cos\theta_X) < 0.15$ GeV^2. In the setup of our experiment, with a 5 cm long liquid hydrogen target, the pure photoproduction (right diagram of Fig.1) contributes only about 25% of the production rate.

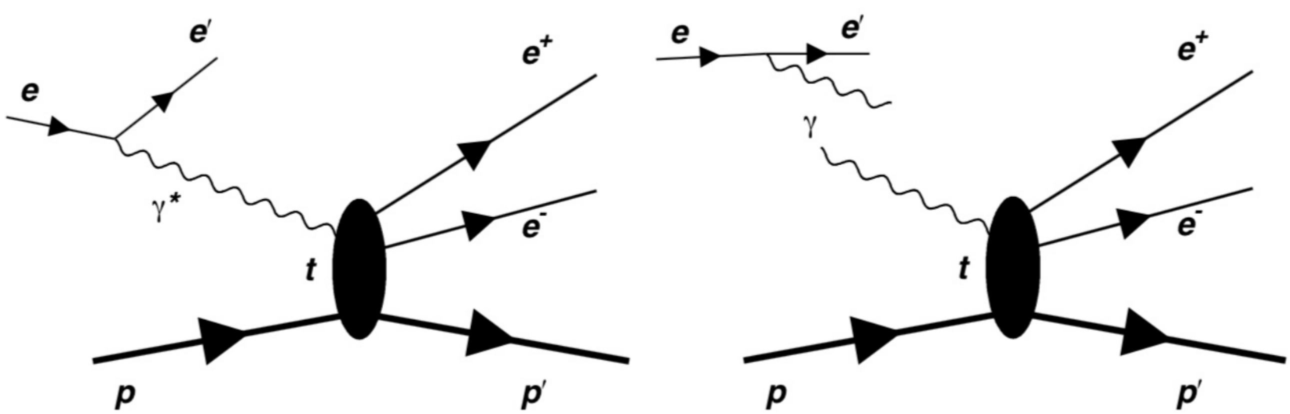

FIG. 1. Diagrams illustrating the electro-(left) and photo-(right) production of an electron-positron pair.

The other kinematical variables used in the analysis are the invariant mass of the lepton pairs:

$$M^2(e^+e^-) \equiv Q'^2 = (\mathrm{k}^+ + \mathrm{k}^-)^2 \tag{3}$$

the energy of the interacting photon:

$$E_\gamma = E_{e^+} + E_{e^-} + E_p - M, \tag{4}$$

were M is the proton mass, and the transferred momentum squared:

$$t = (\mathrm{p} - \mathrm{p}')^2 \tag{5}$$

FORWARD-BACKWARD ASYMMETRY

The forward-backward asymmetry, $\theta \to \pi - \theta$ and $\phi \to \pi + \phi$, exploits the fact that contributions of the Timelike Compton Scattering and Bethe-Heitler processes to the cross section of the lepton pair photoproduction are even under exchange of the lepton charges, whereas the interference term is odd. The latter is simply because the amplitudes for the Compton and BH processes transform with opposite signs in such transformation [1]. In the kinematic domain where the virtuality of the outgoing time-like photon, Q'^2, and the total center of mass energy of (γp), $s = (\mathrm{k}^+ + \mathrm{k}^- + \mathrm{p}')^2$, are large compared to the masses of the proton M and lepton M_l, and the transferred momentum squared $-t$, the angular dependences of the Compton and BH contributions to the cross section are:

$$d\sigma_{BH}(\theta,\phi) \sim \frac{1+\cos^2(\theta)}{\sin^2(\theta)}; \quad d\sigma_{BH}(\theta,\phi) = d\sigma_{BH}(\pi-\theta,\pi+\phi)$$

$$d\sigma_{TCS}(\theta,\phi) \sim \frac{1+\cos^2(\theta)}{4}; \quad d\sigma_{TCS}(\theta,\phi) = d\sigma_{TCS}(\pi-\theta,\pi+\phi)$$

where θ and ϕ are polar and azimuthal angles of the electron in the CM frame of the lepton pair. In the same limit, the angular dependence of the interference term for the leading order and leading twist helicity conserving amplitude, ReM^{--}, is:

$$d\sigma_{INT}(\theta,\phi) \sim \frac{1+\cos^2(\theta)}{\sin(\theta)}\cos(\phi); \quad d\sigma_{INT}(\theta,\phi) = -d\sigma_{INT}(\pi-\theta,\pi+\phi)$$

These relations imply that the forward-backward asymmetry arising from the exchange of the lepton momenta, $\mathbf{k}^- \leftrightarrow \mathbf{k}^+$ will single out the interference term and reads:

$$A_{FB} = \frac{d\sigma(\theta,\phi) - d\sigma(\pi-\theta,\pi+\phi)}{d\sigma(\theta,\phi) + d\sigma(\pi-\theta,\pi+\phi)} = \frac{d\sigma_{INT}(\theta,\phi)}{d\sigma_{BH}(\theta) + d\sigma_{TCS}(\theta)}$$

In the kinematics of this experiment the cross section of the Compton scattering, $d\sigma_{TCS}$, is two orders of magnitude smaller than the one of BH, $d\sigma_{BH}$, and the above expression for A_{FB}, assuming only the leading order and leading twist helicity conserving amplitude, can be written as:

$$A_{FB} \simeq \frac{A}{d\sigma_{BH}} \frac{1+\cos^2(\theta)}{\sin(\theta)}\cos(\phi) ReM^{--}$$

where A is a kinematical parameter.

The CLAS12 acceptance for detection of final state particles in the reaction $\gamma p \to p' e^+ e^-$ at high photon energies is well tailored to study A_{FB}. As shown in Fig.2, due to the forward hole of the spectrometer [2], the detection acceptance in CM frame of the lepton pair at $\phi = 0$ covers the forward polar angular region, $\theta \sim 60°$, while at $\phi = \pi$ it favors to backward polar angles, $\theta \sim 120°$.

RESULTS FOR BSA

The numerical results for the TCS photon polarization asymmetry obtained from the CLAS12 Fall 2018 run dataset are presented in Table I. The asymmetry is calculated as:

$$A_{\odot U}(-t, E\gamma, M; \phi) = \frac{1}{P_b} \frac{N^+ - N^-}{N^+ + N^-}, \tag{6}$$

where the number of events with reported positive N^+ (resp. negative N^-) electron helicity in each bin is corrected by the acceptance (Acc) and the polarization transfer as:

$$N^{\pm} = \sum \frac{1}{Acc} P_{trans.}(E_\gamma). \tag{7}$$

The $A_{\odot U}$ is measured at four transferred momentum squared $-t$. Data are averaged over the photon energy $E_\gamma = 7.29 \pm 1.55$ GeV and the outgoing time-like photon virtuality $2.37 < Q'^2 < 4.24$ GeV^2. In the table, together with the values of $-t$ and BSA, statistical errors and the range of systematic uncertainties are also presented.

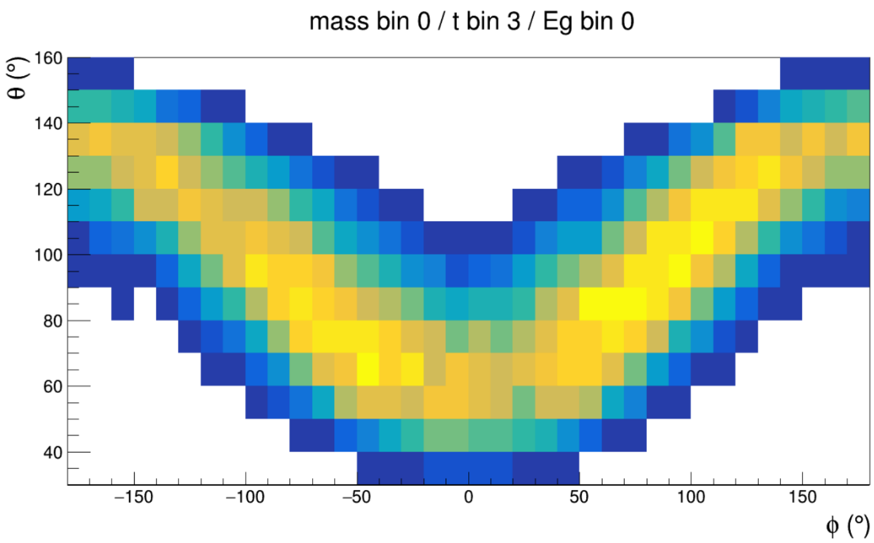

FIG. 2. Acceptance of CLAS12 in the θ/ϕ plane. The region around $\phi = 0°$ and low polar angle, as well as $\phi = \pm 180°$ and high polar angle are well covered by CLAS12.

TABLE I. Photon polarization asymmetry $A_{\odot U}$ as a function of $-t$ at the averaged kinematic point $E_\gamma = 7.29 \pm 1.55$ GeV and $M = 1.80 \pm 0.26$ GeV.

$-t$ (GeV^2)	BSA	Stat. error	Syst. uncert.
0.206	0.166	0.0838	$^{+0.0213}_{-0.0311}$
0.295	0.31	0.0725	$^{+0.0253}_{-0.0439}$
0.404	0.306	0.0656	$^{+0.0224}_{-0.0406}$
0.607	0.177	0.0647	$^{+0.0167}_{-0.0251}$

NUMERICAL RESULTS FOR FB-ASYMMETRY

The forward-backward asymmetry, A_{FB}, was measured for two ranges of the outgoing time-like photon virtualities. A_{FB} is defined as:

$$A_{FB} = \frac{N_F - N_B}{N_F + N_B} \tag{8}$$

where $N_{F/B}$ are the number of events in the forward (backward) angular bins, corrected by the acceptance and the bin volume. In Table II, the measured A_{FB} are shown at four values of transferred momentum squared $-t$. Data are for $2.37 < Q'^2 < 4.24$ GeV^2, averaged over photon energy range $E_\gamma = 7.23 \pm 1.61$ GeV. The A_{FB} for $4.2 < Q'^2 < 6.0$ GeV^2 is presented in Table III. Here the range of photon energies is $E_\gamma = 8.13 \pm 1.23$.

[1] E. Berger, M. Diehl, and B. Pire, Eur. Phys. J. C **23**, 675 (2002).
[2] V. D. Burkert *et al.*, Nucl. Instr. Meth. A **959**, 163419 (2020).

TABLE II. FB asymmetry as a function of $-t$ at the average kinematics $E_\gamma = 7.23 \pm 1.61$ GeV and $M = 1.81 \pm 0.26$ GeV.

$-t(GeV^2)$	A_{FB}	Stat. error	Syst. Uncert.
0.215	0.441	0.175	$^{+0.0442}_{-0.111}$
0.298	0.171	0.0978	$^{+0.044}_{-0.0527}$
0.406	0.27	0.0892	$^{+0.0396}_{-0.0712}$
0.613	0.312	0.102	$^{+0.0406}_{-0.0789}$

TABLE III. FB asymmetry as a function of $-t$ at the average kinematics $E_\gamma = 8.13 \pm 1.23$ GeV and $M = 2.25 \pm 0.20$ GeV.

$-t(GeV^2)$	A_{FB}	Stat. error	Syst. Uncert.
0.288	0.0738	0.178	$^{+0.107}_{-0.11}$
0.395	0.245	0.223	$^{+0.0752}_{-0.136}$
0.49	0.409	0.243	$^{+0.0434}_{-0.171}$
0.658	0.334	0.178	$^{+0.031}_{-0.152}$